JOURNAL OF COLLOID AND INTERFACE SCIENCE **183,** 274–279 (1996)
ARTICLE NO. 0543

Protein Structure Change on Adherence to Ultrafiltration Membranes: An Examination by Electron Paramagnetic Resonance Spectroscopy

S. F. OPPENHEIM,* J. O. RICH,* G. R. BUETTNER,† AND V. G. J. RODGERS*,[1]

*Department of Chemical and Biochemical Engineering, The University of Iowa, 125 Chemistry Building, Iowa City, Iowa 52242; and †ESR and FRRI Center, The University of Iowa College of Medicine, 68 Eckstein Medical Research Building, Iowa City, Iowa 52242

Received March 28, 1996; accepted June 11, 1996

Electron paramagnetic resonance spectroscopy was used to examine changes in the distance between two spin-labels on hen egg lysozyme (HEL, 45 Å × 30 Å × 30 Å, 14,600 Da) when interacting with membranes during ultrafiltration (UF). Membranes with nominal molecular weight cutoff (MWCO) values ranging from 10,000 to 300,000 Da were used. Both cellulosic (hydrophilic) and polysulfone (hydrophobic) membranes were studied. The technique used is based on spin–spin interaction of protein-bound spin-labels that cause dipolar broadening of the EPR spectra. This line broadening is related to spin-label distance and was subsequently used to infer protein conformational changes. The results demonstrate that the distance between the two labels on HEL, while in aqueous solution, was approximately 14.4 Å. Using the known crystal structure of hen egg lysozyme, molecular computer modeling of the doubly labeled protein suggests that the most probable spin–spin distance in solution is 13.9 Å. This distance is in excellent agreement with our experimentally observed result. Protein–membrane interaction reduced this distance approximately by 5 Å, irrespective of the membrane morphology. It is speculated that the lack of variation seen in all the membranes, under our test conditions, may be due to limitations associated with spin-label locations.

Key Words: **EPR; ultrafiltration; spin-label; protein adsorption; protein structure; hen egg lysozyme; line-broadening.**

INTRODUCTION

Considerable attention has been paid to examining the interaction of proteins with various artificial surfaces. Particular attention has been given to polymeric surfaces because of their prevalence in the separation and medical industries (1–6). In those studies, secondary measurements were used to attempt to demonstrate structural changes to the interacting protein. Some of the properties measured were circular dichroism, rotational correlation time, and infrared spectrum of the adsorbed protein (2, 3, 5, 6). In some of these experiments the protein had to be desorbed in order to measure these values, which could alter the results (2).

In membrane separation, protein–surface interaction is also of significant importance. This is primarily because the adsorbed protein can potentially reduce both sieving and permeate flux. However, protein–polymeric interactions during ultrafiltration may also be different from those previously studied. This is primarily because the polymeric membranes are porous, resulting in protein interactions under constricted conditions. In addition, the proteinaceous fluid is driven through the membrane pores by relatively large pressure differences, which may promote protein denaturation.

In this work, we investigate protein–membrane interaction as a result of ultrafiltration. Specifically, we will use spin–spin interaction of doubly spin-labeled hen egg lysozyme (HEL) to discern tertiary conformational changes. This method does not require protein desorption from the membrane material.

SPIN–SPIN INTERACTION AND DISTANCE MEASUREMENTS

Paramagnetic species may interact via dipolar mechanisms. The strength of this interaction is governed by a $(\text{distance})^{-2}$ functionality. This phenomena produces changes in the lineshape and intensities of the EPR spectra. Several studies have taken advantage of these interactions to measure the distance between paramagnetic species (e.g., spin-labels) (7–9). For spin-labels, these methods tend to be viable for distances between ~8 and 27 Å. Two methods used to determine the distance between two spin-labels on a protein from EPR spectra are (1) examination of the half-field line that results from the interaction and (2) simulation of the low-temperature rigid limit EPR spectra produced by the interacting species (7–11). Unfortunately, the half-field EPR line is a result of a forbidden transition. Thus a high concentration of labeled protein is necessitated to produce a high S/N ratio in the EPR spectra. A high ratio is required for successful observation by this method. Our samples did not meet this criteria. Thus in this study we use the rigid limit–line-broadening method (9, 10).

The rigid limit–line-broadening method is less constrained by poor S/N ratios. The rigid limit method assumes

[1] To whom correspondence should be addressed.

0021-9797/96 $18.00

that the labeled molecules with respect to the magnetic field are isotropic. The samples are analyzed at low temperature to minimize dynamic effects. The resulting spectra are input for the unique fitting procedure that yields the width of distribution and interspin distance between the labels (8). The width of distribution is the width of an assumed Gaussian distribution at half intensity. The interspin distance is the average distance value between the labels with a Gaussian distribution assumption.

EXPERIMENTAL

Computer Model

Prior to experimental analysis, a computer model of the doubly spin-labeled HEL was used to determine if the two labels on the test molecule would be within the appropriate range to observe spin–spin interaction by EPR. The X-ray structure of HEL was obtained from the Brookhaven Protein Data Bank and used as the starting structure for all calculations. The doubly labeled HEL model was constructed by attaching 3-maleimidoproxyl moieties to Lys-1 and His-15 of the lysozyme construct using a molecular modeling program (Sybyl 6.2, Tripos Associates, St. Louis, MO, 1995) on a Silicon Graphics Indigo^2 workstation (Mountain View, CA). An algorithm for minimization of molecular energy (Sybyl 6.2) was used to determine that the spin–spin interaction was viable.

A more detailed computer analysis was performed to determine the most probable maximum and minimum spin-label distances that could be expected. A systematic search of the bonds with potential for rotation (three per label–amino acid residue complex) for both labels was performed to elucidate the sterically available conformations. The conformational analysis showed that the spin-label on the His-15 was extremely limited in the available conformations (total possible contribution to the distance between spin label was 0.95 Å). Therefore, the His-15 label was fixed into an appropriate conformation and the label at Lys-1 was adjusted through rotatable bonds RB1, RB2, and RB3 (Fig. 1) in 1°, 2°, and 2° increments, respectively, with a general van der Waals factor of 0.7. The His-15 result is consistent with the work by Wein *et al.* (12) and Schmidt *et al.* (13). The distance between the two free-radicals for the resulting data set (149,829 conformations) was then evaluated in the molecular spreadsheet function of Sybyl.

HEL Purification

HEL (15 kDa, L-6876, Sigma Chemicals, St. Louis, MO) was further purified by gel filtration chromatography. Approximately 1.5 g of Sigma HEL was dissolved in water with pH adjusted to 3 with HCl. This pH was selected to maintain the stability of HEL during purification (14). The solution was injected on to a 4.8 cm × 50 cm low-pressure liquid chromatography glass column (Kontes Chromoflex

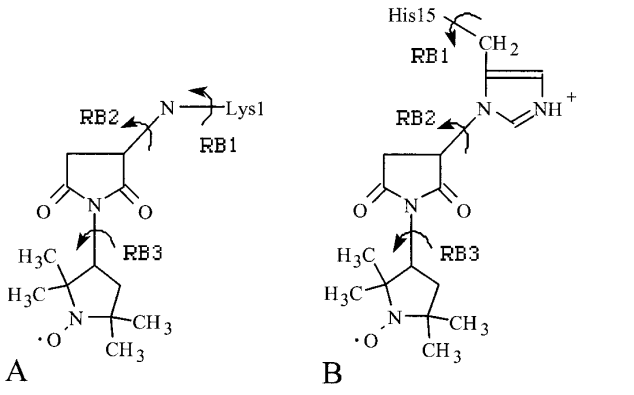

FIG. 1. Schematic representation of the 3-maleimidoproxyl attached to Lys-1 (A) and His-15 (B). The rotatable bonds (distinguished by arrows) RB1, RB2, and RB3 for the Lys-1 label were rotated in 1°, 2°, and 2° increments, respectively. RB1, RB2, and RB3 for the His-15 label were fixed at 204°, 330°, and 28°, respectively.

AQ, Vineland, NJ) containing Toso Haas Toyopearl HW50F beads (Supelco, lot 50HWF79R, Bellefonte, PA). The beads were packed by a constant velocity method. Prior to injection of the sample, the column was flushed with 10 column volumes of water of pH 3 (adjusted with HCl or NH_4OH as needed). The entire separation procedure was controlled by a low-pressure chromatography system (Econo-System, Bio-Rad, Hercules, CA). The eluent was water at pH 3, and the flow rate was 10 ml/min. The eluent was monitored for absorbance at 280 nm and conductance (the HEL peak was indicated by a reduction in conductance and an increase in absorbance at 280 nm). The core of the HEL peak was isolated (~800 ml) and freeze dried.

The large volume prevents shell freezing, therefore the collected HEL peak was passed through a paper filter directly into clean $N_2(l)$. The pellets formed were then removed from the $N_2(l)$ and freeze dried. The resulting product was a fine white powder.

HEL Labeling

The HEL was labeled at Lys-1 and His-15 with 3-maleimidoproxyl using a similar procedure as Likhtenshtein *et al.* (15). Likhtenshtein *et al.* demonstrated that this method resulted in preferential labeling of HEL at these two sites. Upon completing the reaction, the material was ultrafiltered with water at pH 3 for 10 cell volumes using a 10,000 MWCO cellulosic membrane. Afterward the retentate was freeze dried to produce a white powder. The doubly spin-labeled HEL (DL-HEL) was examined and found to have approximately 2.4 ± 0.07 labels. This is consistent with the spin-label count observed by Likhtenshtein *et al.*

Singly labeled HEL (SL-HEL) was also produced to determine overall mass uptake on the selected membranes. For this, the spin-label 3-(2-bromoacetamido)proxyl (15) was used. The protein preparation was the same as described above.

Procedures for Estimating Distance between Spin-Labels

The distance estimation procedure can be divided into two parts. First, the magnetic hyperfine tensor **A** is determined for the label being used. Evaluation of the magnetic elements of **A** (i.e., A_{xx}, A_{yy}, A_{zz}) requires that the labels be at a distance apart where they are not interacting with one another. The availability of the resulting tensor facilitates distance calculations by reducing the number of parameters to be fitted. After these tensors are obtained, the distance experiments and analysis can be performed.

Obtaining Hyperfine Magnetic Tensors

EPR analysis. DL-HEL was dissolved in a solution of 8 *M* urea and 6.7 vol% of Triton X-100. This mixture serves two purposes. First, it denatures the protein. This allows the labels to be at their extreme distance, thereby reducing label interaction. Second, it aids in getting the solution to wet the carrier material. The carrier used was polypropylene nonwoven material used for the membrane backing in this study (Millipore, F02430, lot 11036PP, Bedford, MA). The low-temperature EPR setup developed by Oppenheim *et al.* (6) for ultrafiltration membranes was used. The membrane backing was first wetted with 25 μl of protein solution. Then, the backing was wrapped around a Wilmad 3 mm o.d. quartz EPR tube and placed in a low-temperature cavity setup (standard cavity, Bruker ER411VT low-temperature unit). All EPR spectroscopy was performed with a Bruker ESP 300 spectrometer (Billerica, MA). Typical parameters were as follows: modulation amplitude, 1 G; time constant, 82 ms; receiver gain, 2.5×10^4; scan width, 120 G; power 20 mW; frequency, 9.42 GHz; scan center, 3475 G; and number of scans, 50. The sample was scanned at 100 K, and the spectra were recorded.

The hyperfine tensor is affected by the hydrophobic/hydrophilic nature of its environment. Therefore to take into account any differences due to the physical setup, the denatured DL-HEL solution was also examined separately as a frozen solution in a 5 mm quartz EPR tube. Five samples were analyzed, and the **A** tensor elements and lineshape parameters were obtained.

Computation. As part of this analysis an assumption was made that these tensors and lineshape parameters were the same as those related to the distance measurement analysis. The computational details are given below.

Obtaining Distance Values

EPR analysis. The test solution contained 0.1% HEL in a pH 4.5, 0.15 *M* citrate, phosphate-buffered saline containing 0.02% NaN_3 as a preservative. This pH was selected to minimize potential dimerization of HEL (13). A total of 15% of the HEL was DL-HEL. A stirred batch cell was used as the test cell (UHP 43, Cole Parmer, Vernon Hills, IL). Prior to exposure, the hydraulic permeabilities of the test membranes were obtained using deionized water. The test membranes were 44 mm in diameter; 10,000 MWCO polysulfone (PTGC, lot P3NM8372, Millipore), 30,000 MWCO polysulfone (PTTK, lot P4BM8442, Millipore), 300,000 MWCO polysulfone (PTMK, lot P4PM0209, Millipore), and 30,000 MWCO cellulose (PLTK, lot P3EM7199, Millipore) membranes (6). These membranes were selected to provide a range of protein–membrane interactions, with polysulfone having high potential for hydrophobic adsorption and cellulosic membranes having high hydrophilic interaction. The pore sizes selected span the range of separation from little retention (300,000) to partial retention (30,000) to high retention (10,000).

Following hydraulic permeability examination, the protein solution was ultrafiltered with the prescribed membranes for 1 h at 34.5 kPa (gauge) and 500 rpm in the stirred batch cell. After exposure the membranes were washed with deionized water for 10 min at 0 kPa. The hydraulic permeability was then checked after washing. A 12 mm $\times$ 39 mm sample was removed and examined using EPR as described above.

The solution was also examined in 5 mm i.d. quartz EPR tube. The spin-label distance measurements were determined for solution using the solution parameters as found using the methods described above.

Computation. The spectra were analyzed by the rigid limit–line-broadening program developed by Steinhoff (9) using the **A** tensor and lineshape parameters. In all cases, three samples were used and all cases converged. The FORTRAN program was compiled and run on a 486 platform using Microsoft FORTRAN version 5.1.

Determining Mass Uptake

A solution was prepared containing 0.1% SL-HEL with a total HEL concentration of 5% in a pH 4.5, 0.15 *M* citrate, phosphate-buffered saline containing 0.02% NaN_3 as a preservative. Ultrafiltration of the SL-HEL containing solution was conducted with the tests membranes under the same conditions described above. The initial and final hydraulic permeabilities of the membrane were determined.

Afterward the membranes were examined in the Bruker ESP 300E spectrometer using the Wilmad quartz tissue cell. Typical parameters were as follows: modulation amplitude, 1 G; time constant, 82 ms; receiver gain, 2.5×10^4; scan width, 120 G; power 20 mW; frequency, 9.73 GHz; scan center, 3455–3461 G; cavity, TM_{110}; temperature, 293 K; and number of scans, 50. The resulting spectra were double integrated and compared to a prepared calibration curve to determine mass uptake of SL-HEL. The ratio of total HEL to SL-HEL was used to determine the total lysozyme mass uptake on the membranes. It was previously shown that SL-HEL is not preferentially adsorbed on the membranes used in this study (6). All samples were studied in duplicate and averaged.

TABLE 1
Magnetic Tensors Used for Distance Analysis

	A_{xx} (G)	A_{yy} (G)	A_{zz} (G)
Membrane	2.91 ± 0.91	1.66 ± 1.18	35.6 ± 0.63
Solution	1.90 ± 0.68	3.75 ± 0.30	32.7 ± 0.14

RESULTS AND DISCUSSION

The computation study for the minimization of energy algorithm indicated that variations in the tertiary structure of the protein can result in the two labels being as close as 9 Å and as far apart as 23 Å in a native type environment. A more detailed analysis using the algorithm for determining the most probable spin-label distance showed that the maximum and minimum distances were 23.7 and 8.9 Å, respectively. These values fell within the range that is accessible to experimental distance analysis. The more detailed analysis for the most probable spin-label distances indicated that the average distance between the oxygen of the nitroxide radical moieties on Lys-1 and His-15 spin-labels would be 13.9 Å.

Using the experimental determined hyperfine tensor for DL-HEL in solution (Table 1), the Steinhoff distance computation method was carried out. This line-broadening method yielded an experimental spin–spin distance of 14.4 ± 0.5 Å, which is in remarkable agreement with the Sybyl prediction. Further, the Steinhoff spectral fitting, the basis of the distance calculation, is in close agreement with the experimental spectra (Figs. 2 and 3). The consistent distance measurements from the line-broadening method and the computer simulation of spin labeled Lys-1 and His-15 help further support the spin-label locations.

The homogeneous solution experiments with DL-HEL described above have demonstrated the viability of the EPR approach for determination of intramolecular distance. To determine if intramolecular protein distance changed upon interaction with ultrafiltration membranes, the EPR, double-label approach was applied to membrane samples with adsorbed DL-HEL. The experimental spin-label distances for protein–membrane interaction are all approximately 5 Å below the distance value found in homogenous solution of DL-HEL (Fig. 3). On the basis of the size of the HEL molecule and the original distance between the labels, this is a considerable size variation due to membrane interaction. However, it was unexpected to have all membrane samples, with significant difference in hydrophobicity and pore size, behave so similarly.

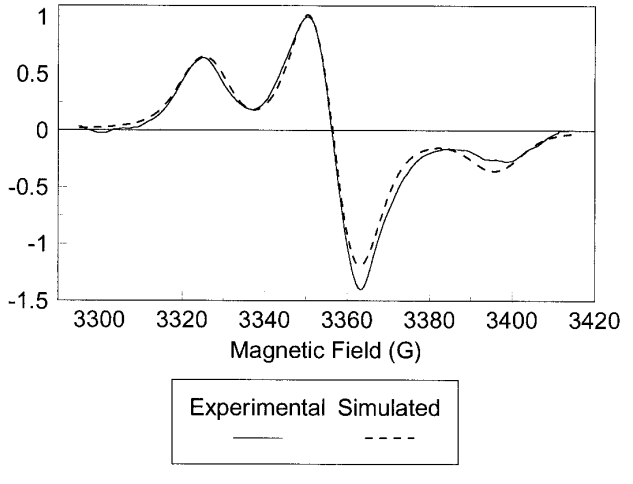

FIG. 2. Comparison of experimental, solution EPR spectrum to spectrum generated by distance analysis program.

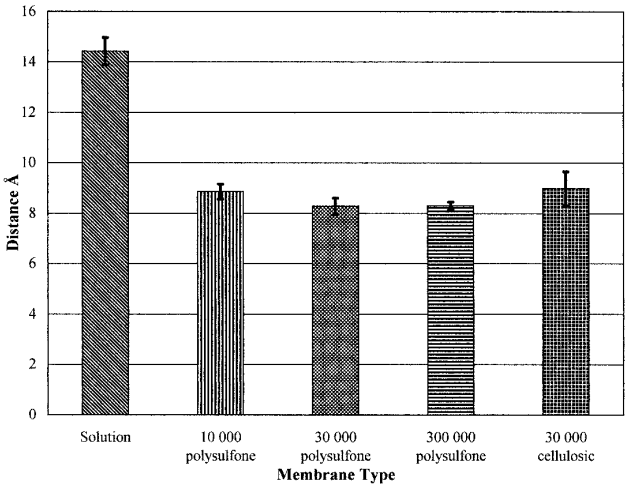

FIG. 3. Distance measurements of HEL on various ultrafiltration membranes.

It was expected that the polysulfone membrane–protein interaction would initiate protein denaturation, because the hydrophobic adsorption is entropically driven (16). As a result, we hypothesized that the resulting protein denaturation would be reflected in differences in the spin-label distances between the hydrophobic polysulfone membranes and the highly hydrophilic cellulosic membranes. However, the spin–spin distance measurements for DL-HEL adsorbed on polysulfone or cellulosic membranes are similar. These results can be due to a number of reasons, including that the conformational changes in tertiary structure are similar for different interactions, or that the structural changes are due to a common more dominant adsorption mechanism.

An alternative adsorption force that is prevalent is electrostatic interaction. Initial protein adsorption has been shown to be dominated by electrostatic interactions, particularly when the ζ potential of the macromolecule and the membrane are oppositely charged, although electrostatic interaction can be significant even when proteins and membranes have the same net charge (17). In this study lysozyme, with an isoelectric point of pH 11.2, is highly positively charged at pH 4.5, and both polysulfone and cellulosic membranes are expected to be near neutral or have a slightly negative charge under our experimental conditions (18–21). The ac-

TABLE 2
Mass Uptake and Estimated Properties of Membranes Ultrafiltered with SL-HEL for 1 h

Membrane material	Pore size (Da)	Mass HEL (mg)	Initial L_p (m s^{-1} kPa^{-1} $\times$ 10^{14})	Final L_p (m s^{-1} kPa^{-1} $\times$ 10^{14})	q_s
Polysulfone	10,000	0.128 ± 0.011	4.68 ± 0.43	2.51 ± 0.047	0.14
Polysulfone	30,000	0.833 ± 0.202	9.92 ± 0.70	6.18 ± 0.91	0.11
Polysulfone	300,000	0.272 ± 0.017	215 ± 17.3	42.1 ± 0.2	0.33
Cellulosic	30,000	0.034 ± 0.006	4.48 ± 0.58	4.07 ± 0.32	0.02

tual value of the ζ potential for the membranes is a function of the solution pH, ionic strength, and presence of protein (19–21).

If electrostatic interaction is the dominant interaction for both membrane materials, it is expected that the amount of surface coverage should be equivalent. Table 2 shows the total mass of HEL for the membranes. In addition, the fraction of pore void volume of the membrane occupied by protein, q_s, was also determined assuming a cylindrical pore model (22). Comparing the polysulfone and cellulosic 30,000 MWCO membranes shows that there is an increase of nearly 25 times more protein on the polysulfone membrane. Using the relationship

$$\frac{S_{p,polysulfone}}{S_{p,cellulosic}} = \left(\frac{L_{p,cellulosic}}{L_{p,polysulfone}}\right)^{1/2} \left(\frac{\epsilon_{polysulfone}}{\epsilon_{cellulosic}}\right)^{3/2}, \qquad [1]$$

where S_p is the membrane pore surface area, L_p is the membrane initial hydraulic permeability, and ϵ is the membrane void fraction, the difference in the available pore surface area can be estimated. Using the conservative assumption that the respective void fractions are equivalent, the ratio of available surface area is 2/3 for polysulfone versus cellulosic membranes. Clearly, the polysulfone membrane has substantially more protein surface coverage. This significant difference in surface coverage between these similar pore sized membranes implies that the dominant adsorption mechanisms for the respective membranes are different. Therefore it is unlikely that the similarity in the distance measurements are the result of the same dominant adsorption mechanisms. It may be possible that the doubly spin-labeled protein underwent similar tertiary structural changes for different dominant adsorption mechanisms. HEL is regarded as a highly stable molecule due to its four disulfide bonds, and it may therefore be limited during denaturation.

The half-width distribution for the spin–spin distances should provide a window into the heterogeneity/homogeneity of the global environment of the protein. The half-width distributions determined by the rigid limit–line-broadening method of DL-HEL interaction various membranes are the same (Fig. 4). For a Gaussian distribution, the half-width would represent about 2.4 times the standard deviation, σ. Thus σ is about 2.5 Å for each of the membrane samples. This standard deviation implies a more heterogeneous environment for the adsorbed states than observed in solution.

The spin-labels are not symmetrically located on HEL; if it is assumed that the adsorption site interaction of the protein with the membrane is on a scale much smaller than the overall size of the protein, then this observation implies that the HEL is taking on a specific orientation as it interacts with the membrane. Previous research has shown that other proteins such as albumin, ribonuclease A (RNase A), γ-globulin, and fibrinogen select a specific orientation on many polymeric surfaces during both highly electrostatic and hydrophobic adsorption (16, 17, 23). For the interaction of RNase A with negatively charged mica, it was postulated that the initial orientation of the macromolecule was such that positively charged active sites were aligned with the charged surface.

The above analysis demonstrates some of the limitations in interpreting spin–spin interaction distance of doubly spin-labeled macromolecules. However, to further utilize spin-label distance measurements to appreciate protein denaturation during ultrafiltration, triply spin-labeled HEL or other protein may be used. In addition to Lys-1 and His-15, lysozyme can also be labeled at Asp-52. Literature suggests that such labeling is possible (15). Asp-52 is on the opposite side of Lys-1 and His-15, in the active site, and yet remains

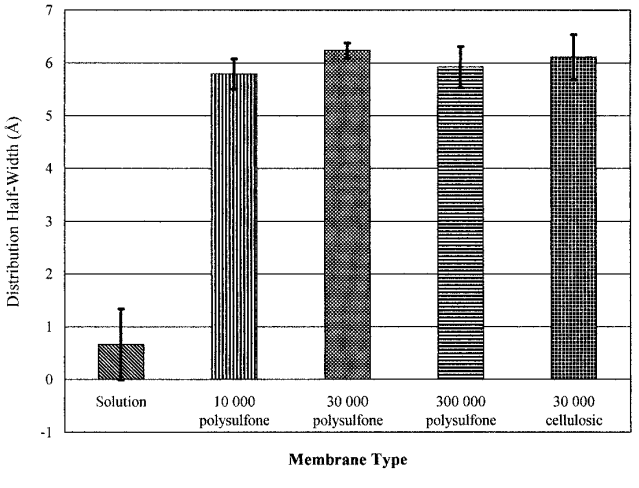

FIG. 4. Half-width distribution of HEL on various ultrafiltration membranes.

in the bounds of the detectable distance between the other labeled sites. Thus, the resulting analysis may provide significantly more information on protein structure variations. The rigid limit–line-broadening approach (8) can be modified to provide distances between three labels.

In previous work, we demonstrated that the rotational correlation times for the spin-labels have excellent correlation with the type of adsorption and steric hindrance experienced by the macromolecule under similar experimental conditions (6). Thus, the rotational correlation time is notably more sensitive to these property variations. This may be because the rotational correlation time is based on the highly localized region of the spin-label in the protein rather than on the environment of the entire macromolecule.

This preliminary research demonstrates promise in analyzing protein denaturation on highly porous amorphous surfaces. It also allows one to determine the impact of ultrafiltration (such as pressure contributions and shear stress in the pores) on the denaturation process. However, in this study, the variation in distance measurements with respect to porous structure for the polysulfone membranes (Fig. 3) is negligible. This may be due to factors cited above for limited variability in distance measurements for different adsorption states. Future studies will include using membranes not subject to ultrafiltration as controls and reducing the electrostatic interaction of the system. This will aid in discerning the impact of pore size and ultrafiltration operating conditions.

CONCLUSIONS

A method has been introduced to use distance shifts in spin-labels on HEL to infer conformational changes of the protein as a result of protein–membrane interaction and ultrafiltration conditions. The spin-label distance measurement for the protein in solution was consistent with the distance value generated by molecular modeling. The method presented showed a clear difference between distance measurements between the protein in solution and the protein interacting with the membrane. Despite the fact that both hydrophobic and hydrophilic membranes were used, the spin-label values for these membranes are similar. It is postulated that this may be due to the limited detection of more significant structural changes of the protein outside of the region between the two spin-labels or similar distance changes that occur due to the rigid structure of the HEL molecule. For similar reasons, the pore size variation did not introduce any additional changes in the spin-label distance between the membrane cases. Future research will incorporate triply spin-labeled protein to determine structural changes.

APPENDIX: NOMENCLATURE

$\mathbf{A}$	hyperfine magnetic tensor (G)
A_{pp}	hyperfine magnetic tensor element (G)
L_p	hydraulic permeability (m s^{-1} kPa^{-1})
q_s	fraction of pore volume occupied by protein
S_p	pore surface area
ϵ	void fraction of membrane
σ	standard deviation
pp	xx, yy, zz directional indication of the hyperfine magnetic tensor element

ACKNOWLEDGMENTS

The authors thank Heinz-Jurgen Steinhoff and Nicole Radzwill for the use of the rigid limit–line-broadening distance determination program. The authors also thank the Millipore Corporation for samples of their membrane backing material. This work has been financially supported by USDA Grant 416-20-03.

REFERENCES

1. Eirich, F. R., *J. Colloid Interface Sci.* **58,** 423 (1977).
2. Soderquist, M. E., and Walton, A. G., *J. Colloid Interface Sci.* **75,** 2 (1980).
3. Tan, J. S., and Martic, P. A., *J. Colloid Interface Sci.* **136,** 415 (1990).
4. Shirahama, H., Lyklema, J., and Norde, W., *J. Colloid Interface Sci.* **139,** 177 (1990).
5. Lu, D. R., and Park, K., *J. Colloid Interface Sci.* **144,** 271 (1991).
6. Oppenheim, S. F., Buettner, G., and Rodgers, V. G. J., *J. Membr. Sci.*, in press (1996).
7. Eaton, S., More, K., Sawant, B., and Eaton, G., *J. Am. Chem. Soc.* **105,** 6560 (1983).
8. Farahbakhsh, Z. T., Huang, Q. L., Ding, L. L., Altenbach, C., Steinhoff, H. J., Horwitz, J., and Hubbell, W. L., *Biochemistry* **34,** 509 (1995).
9. Steinhoff, H. J., *Biochem. Biophys. Meth.* **78,** 237 (1988).
10. Steinhoff, H. J., Dombrowsky, O., Karim, C., and Schneiderhahn, C., *Eur. Biophys. J.* **20,** 293 (1991).
11. Rabenstein, M. D., and Shin, Y. K., *Proc. Natl. Acad. Sci. U.S.A.* **92,** 8239 (1995).
12. Wein, R. W., Morrisett, J. D., and McConnell, H. M., *Biochemistry* **11,** 3707 (1972).
13. Schmidt, P. G., and Kuntz, P. G., *Biochemistry* **23,** 4261 (1984).
14. Redfield, C., and Dobson, C. M., *Biochemistry* **27,** 122 (1988).
15. Likhtenshtein, G. I., Akmedov, Y. D., Ivanov, L. V., Krinitskaya, L. A., and Kokhanov, Y. V., *Mol. Biol.* **8,** 40 (1975).
16. Soderquist, M. E., and Walton, A. G., *J. Colloid Interface Sci.* **75,** 386 (1980).
17. Norde, W., *Colloids Surf.* **10,** 21 (1984).
18. Tanford, C., and Wagner, M. L., *J. Am. Chem. Soc.* **76,** 3331 (1954).
19. Nystrom, M., Pihlajamaki, A., and Ehsani, N., *J. Membr. Sci.* **87,** 245 (1994).
20. Elimelech, M., Chen, W. H., and Waypa, J. J., *Desalination* **95,** 3, 269 (1994).
21. Lee, C. K., and Hong, J., *J. Membr. Sci.* **39,** 79 (1988).
22. Rodgers, V. G. J., Oppenheim, S. F., and Datta, R., *AIChE J.* **47,** 1826 (1995).
23. Lee, C.-S., and Belfort, G., *Proc. Natl. Acad. Sci. U.S.A.* **86,** 8392 (1989).